J. Heat Treating (1990) 8:81–91


# Prediction of the Temperature–Time Cooling Curves for Three-Dimensional Aluminum Products during Spray Quenching

**T.A. Deiters and I. Mudawar**

**Abstract.** This study aims at developing a universal approach to predicting the temperature–time characteristics for three-dimensional aluminum parts during quenching with water sprays. The validity of correlations recently developed by one of the authors, which relate the local heat transfer rate to the spray hydrodynamic parameters, is examined for nonuniform sprays. A mathematical relation is presented for characterizing the spatial distributions of the hydrodynamic parameters. By combining the local heat transfer correlations with the spatial distribution equations of these parameters, it is shown how a spatial distribution of the surface heat transfer rate can be derived. This distribution provides the vital boundary conditions needed to numerically simulate the three-dimensional heat diffusion occurring in a spray cooled part and the resultant temperature–time cooling curve at every point in the part. The validity of this approach is demonstrated by comparing numerical predictions with experimental measurements on a three-dimensional rectangular aluminum block subject to a nonuniform spray cooling boundary.

## Nomenclature

| | | |
|---|---|---|
| $A_i$ | = | empirical constant |
| $c_p$ | = | specific heat |
| $d$ | = | drop diameter |
| $d_{32}$ | = | Sauter mean diameter |
| $h_{fg}$ | = | latent heat of vaporization |
| $k$ | = | thermal conductivity |
| $l$ | = | nozzle to surface distance |
| $n$ | = | number of drops of a particular diameter in a spray sample |
| $N$ | = | total number of drops in a spray sample |
| $Nu_{32}$ | = | Nusselt number based on Sauter mean diameter, $(h\ d_{32}/k)$ |
| $P$ | = | nozzle upstream pressure |
| $Pr$ | = | Prandtl number |
| $q''$ | = | heat flux |
| $q''_{\max}$ | = | critical heat flux |
| $Q''$ | = | volumetric spray flux |
| $Re_{32}$ | = | Reynolds number based on volumetric spray flux and Sauter mean diameter, $(Q''d_{32}/\nu_f)$ |
| $t$ | = | time |
| $T$ | = | temperature |
| $T_{\text{Leid}}$ | = | Leidenfrost temperature |
| $T_{\max}$ | = | surface temperature corresponding to $q''_{\max}$ |
| $\Delta T_s$ | = | $T_s - T_f$ |
| $\Delta T_{\text{sub}}$ | = | $T_{\text{sat}} - T_f$ |
| $u$ | = | drop velocity normal to the quench surface |
| $U_m$ | = | mean drop velocity normal to the quench surface |
| $X$ | = | distance measured along length of aluminum block |

T.A. Deiters is Graduate Research Assistant and I. Mudawar is Director of the Boiling and Two-Phase Flow Laboratory, School of Mechanical Engineering, Purdue University, West Lafayette, IN 47907, USA.

$Y$ = distance measured along width of aluminum block
$Z$ = distance measured along height of aluminum block from quench surface

*Greek Symbols*

$\alpha$ = thermal diffusivity
$\nu$ = kinematic viscosity
$\rho$ = density
$\sigma$ = surface tension
$\Psi$ = variable representing predicted value of $Q''$, $d_{32}$, or $U_m$

*Subscripts*

$f$ = liquid
$g$ = vapor
$i$ = particular measurement in a spray sample
Leid = Leidenfrost
max = critical heat flux (CHF)
$s$ = surface
sat = saturated
sub = subcooled

## Introduction

Cost-effective fabrication of heat treated aluminum has led to the development of "press quenching" for the final cooling step of extruded alloys. During press quenching, the alloy is cooled by a deluge of water sprays immediately after exiting the die. Mechanical and metallurgical requirements impose limits on the rates at which aluminum alloys can be quenched by water sprays. The upper limit is set by the occurrence of plastic deformation which causes warping of the product, and the lower limit is set by an inability to develop the required metallurgical properties in subsequent heat treatment operations. In addition, if a product contains sections of differing thicknesses, it is unlikely that the optimum properties or desired final shape can be obtained throughout the cross section using sprays having the same flow rate [1]. At present a method for determining the spray nozzle location with respect to the surface and the volumetric flux (volume flow rate per unit area) required for cooling a given alloy and geometry is not available, and this causes much guesswork and trial and error in establishing an acceptable configuration for a production run. This day-to-day variation in quality usually results in a costly posttreatment consisting of additional heat treatment and straightening in order to meet product specifications. For example, it is estimated that 50% of the cost of posttreatment of aluminum extrusions is due to stresses thermally induced during the press quenching process.

It is crucial that a method for optimizing the cooling rate for spray quenched aluminum parts based on their shape and desired metallurgical properties be developed if production cost is to be reduced and product quality to be improved. A schematic of such a method is shown in Figure 1. This method involves the synthesis of heat transfer and metallurgical data bases via a Computer Aided Design (CAD) system [1]. It is envisioned that a design engineer would submit the part specifications to the production engineer and would then utilize the metallurgical data base to determine the optimum cooling rate using the CAD system. Following a series of iterations utilizing its heat transfer data base, the CAD system would select a spray cooling configuration that would provide acceptable temperature–time cooling characteristics at every point in the quenched part and output the results in the form of nozzle types, locations, and operating pressures. The production engineer would then configure the spray chamber according to these recommendations. It is not too far-sighted to consider having a microprocessor robotically control the spray nozzle positions and operating pressures.

Even without the robot control this process provides many benefits to the metal fabrication industry. Initially, it will significantly decrease the costly setup time and reduce the scrap resulting from the trial and error method of finding the correct quench rate. During production, it would also provide consistent material properties by inhibiting the variability of product quality associated with day-to-day human decisions, and virtually eliminate the posttreatment of the part to correct any distortions that may have occurred during the quench. Additionally, this pro-

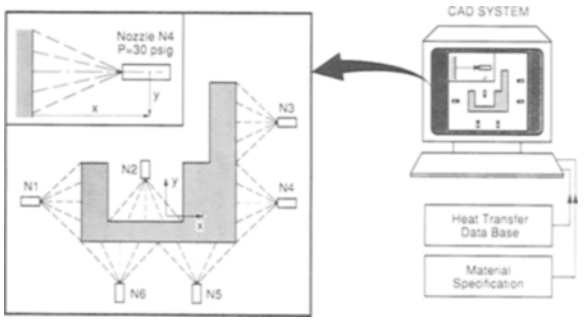


**Fig. 1.** Schematic representation of the intelligent spray quenching system [1].

cess is well suited for small batch operations where pre- and postproduction costs are not as easily recovered in the volume of parts produced.

At the present time, a complete heat transfer data base for spray quenching is not available. If the ultimate goals of improving metallurgical and mechanical properties and reducing thermal stresses during spray quenching are to be achieved, then research must be conducted that would characterize the heat transfer aspects of quenching and facilitate predicting the temperature–time cooling characteristics at every point in the part.

The open literature includes findings from many spray cooling studies which were aimed at either developing a fundamental understanding of the heat transfer mechanisms associated with the impingement of spray drops on a preheated surface, or the practical design methodology for optimizing the spray cooling process. A comprehensive literature review by Brimacombe et al. [2] leads to the conclusion that volumetric spray flux, $Q''$ has the strongest effect on the heat transfer rate during a quench, but there is much debate and confusion concerning the effects of secondary parameters such as surface temperature [3, 4, 5], nozzle exit velocity [6], nozzle to surface distance [7] and the spatial nonuniformity in heat flux attributed to these secondary effects. Reiners et al. [8] measured a 2000 W/m$^2$ · K variation in the heat transfer coefficient over a distance of only 100 mm, and demonstrated that spatial nonuniformity increases with increasing volumetric spray flux.

Most of the studies on spray quenching have been focused on the cooling of steel from very high temperatures. Consequently, most of the conclusions drawn from these studies pertain to the *film boiling* regime, a slow cooling process characterized by the formation of a thermally insulating vapor layer between the liquid and the surface. This vapor layer is interrupted by partial wetting of the surface at the *Leidenfrost* point, the lowest temperature corresponding to the film boiling regime, following which quenching proceeds at a much faster rate. In the spray cooling of aluminum alloys, the surface temperature at the onset of the quench ($T_s \leqslant 525°$ C) may only be slightly higher than the Leidenfrost temperature and, with some powerful sprays, even lower than the Leidenfrost temperature. It is thus necessary that the entire quench (boiling) curve be characterized for spray cooling of aluminum especially in the boiling regimes involving wetting of the surface (i.e., transition boiling and nucleate boiling) and, to a lesser extent, the low temperature liquid cooling regime.

**Table 1.** Mudawar and Valentine's [9] Spray Quenching Correlations

| Boiling (Quenching) Regime | Correlation[a,b] |
|---|---|
| Leidenfrost heat flux | $\frac{q''_{\text{Leid}}}{\rho_g h_{fg} Q''} = 0.145 \left(\frac{U_m}{Q''}\right)^{0.834}$ |
| Transition boiling | $\log_{10}\left(\frac{q''}{q''_{\max}}\right) = 4.78 \times 10^5 \left(\frac{U_m}{Q''}\right)^{-1.255} \left[\log_{10}\left(\frac{T_s - T_f}{T_{\max} - T_f}\right)\right]^3 - 1.90 \times 10^4 \left(\frac{U_m}{Q''}\right)^{-0.903} \left[\log_{10}\left(\frac{T_s - T_f}{T_{\max} - T_f}\right)\right]^2$ |
| Critical heat flux | $\frac{q''_{\max}}{\rho_g h_{fg} Q''} = 122.4 \left[1 + 0.0118 \left(\frac{\rho_g}{\rho_f}\right)^{1/4} \left(\frac{\rho_f c_{pf} \Delta T_{\text{sub}}}{\rho_g h_{fg}}\right)\right] \left(\frac{\sigma}{\rho_f Q''^2 d_{32}}\right)^{0.198}$ <br> $T_{\max} = 18 \left[(\rho_g h_{fg} Q'') \left(\frac{\sigma}{\rho_f Q''^2 d_{32}}\right)^{0.198}\right]^{1/5.55} + T_f$ |
| Nucleate boiling | $q'' = 1.87 \times 10^{-5} (T_s - T_f)^{5.55}$ |
| Incipient boiling | $T_s = 13.43\, Re_{32}^{0.167}\, Pr_f^{0.123} \left(\frac{k_f}{d_{32}}\right)^{0.220} + T_f$ |
| Single phase | $Nu_{32} = 2.512\, Re_{32}^{0.76}\, Pr_f^{0.56}$ |

[a] The units of the parameters used in these correlations are: $q''$(W/m$^2$), $d_{32}$ (m), $k$(W/m · K), $T(K)$, $U_m$ (m/sec) and $Q''$ (m$^3$ sec$^{-1}$/m$^2$).
[b] Ranges of experimental parameters associated with the development of these correlations are: $Q''$ = 0.60–9.96 m$^3$ sec$^{-1}$/m$^2$, $d_{32}$ = 405–1351 μm, $U_m$ = 10.9–26.7 m/sec and $T_f$ = 23–80° C.

During the last four years, an investigation into the heat transfer aspects of quenching has been conducted at the Purdue University Boiling and Two-Phase Flow Laboratory. In a subtask of this effort, Mudawar and Valentine [9] generated heat transfer correlations for spray cooling which were based upon *local* values of three hydrodynamic spray parameters: volumetric spray flux, mean drop diameter, and mean drop velocity. These correlations are universal to all types of sprays and believed to be spatially independent since they are defined with respect to the local spray hydrodynamic parameters upon impingement onto the heated surface rather than upstream conditions such as nozzle pressure, nozzle exit velocity, or nozzle-to-surface distance. Correlating data with respect to the latter parameters both renders the correlation dependent upon the specific type of spray (e.g., full-cone hollow-cone, or flat spray), and preclude the determination of spatial variations in the heat transfer rate. Table 1 shows a summary of the heat transfer correlations developed by Mudawar and Valentine and details the range of values for each of the hydrodynamic parameters associated with these correlations.

The present study is a continuation of the work by Mudawar and Valentine and constitutes the second step in the development of the optimized spray quenching system represented in Figure 1. Using Mudawar and Valentine's correlations between the local heat transfer rate and local spray hydrodynamic parameters, the present study examines how these parameters are distributed in a spray field, thus building the critical bridge from local to global determination of the heat transfer rate associated with spray cooling. This paper presents a systematic technique for predicting the temperature–time cooling characteristics at any point in a three-dimensional part and demonstrates the feasibility of this technique by comparing numerical prediction with experimental measurements on a three-dimensional rectangular aluminum block subject to nonuniform spray cooling on one side.

## Experimental Techniques

The three main objectives of the present study are (a) to verify experimentally that the correlations developed by Mudawar and Valentine are indeed spatially independent, (b) to characterize the distributions of the spray hydrodynamic parameters and (c), to couple these distributions with the local heat transfer correlations to predict the spatial distribution of the heat transfer rate from the quench surface of a three-dimensional part. These objectives demanded three separate experimental measurements as detailed in the following sections.

### *Local Heat Transfer Measurements*

Local heat transfer measurements were obtained at various points within the spray field using a heating device which measures surface temperature and surface heat flux simultaneously. A steady state method was employed in these measurements to ensure the acquisition of accurate spray boiling data, especially near the critical boiling heat flux, $q''_{max}$, where the cooling rate from the surface is at a maximum. This method involves balancing the heat transfer rate to the spray with energy supplied at a steady rate from a resistive electrical element embedded in the heating device, thus maintaining steady state conditions corresponding to any point along the quench curve for the duration of data acquisition.

The surface (quench) area of the heating device had to be small enough to ensure sensitivity of the measurement to spatial gradients in the heat flux. Both aluminum and copper heating devices were fabricated with quench areas of 0.50 cm$^2$ as shown in Figure 2. The thermocouples in the neck of the device provided a temperature gradient which was used to extrapolate the surface temperatures as well as to determine the surface heat flux. Both materials measured identical boiling curves due to their high thermal conductivities as demonstrated previously by Mudawar and Valentine [9] and Baumeister and Simon [10]. Initial experiments proved the temperature in the aluminum heating device in the vicinity of the resistive element was well above original estimates due to the high heat fluxes associated with water sprays. Since pure copper is more resistant to

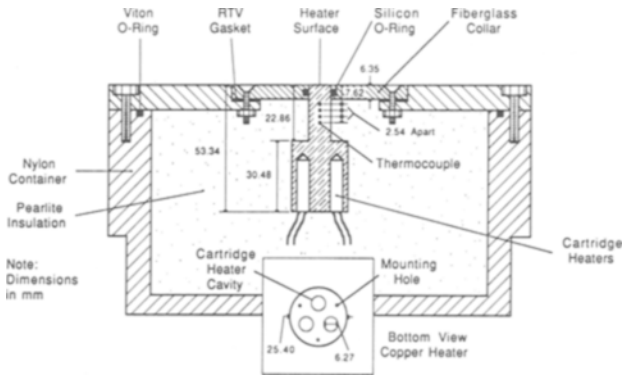


**Fig. 2.** Schematic diagram of the heating device used for obtaining local measurements in the spray field.

oxidation and capable of withstanding higher temperatures compared to aluminum, copper was used exclusively for the local heat transfer measurements of the present study. The oxygen-free copper maintained a nearly constant thermal conductivity of 392 W/m·K over the operating range of interest. The reader is referred to the paper by Mudawar and Valentine for details concerning the accuracy of the heat transfer measurements and the validity of developing boiling correlations for aluminum and other conductive materials based upon measurements obtained with the copper heating device.

### *Measurement of Volumetric Spray Flux, Drop Diameter and Drop Velocity*

Measurement of the volumetric flow rate, $Q''$, was performed with the aid of a 200 ml graduated cylinder having an inlet area of 1.0 $cm^2$. The heating device was removed from the test bracket and the cylinder mounted on the bracket so that the inlet to the cylinder was at the same location as the surface of the heating device. The time required to fill the cylinder was measured, and $Q''$ was calculated by dividing the volume of water in the cylinder by the fill time and the area of the cylinder inlet. The local spray flux measurements ranged from near zero just outside of the spray boundary to a maximum of $3 \times 10^{-3}$ $m^3$ $sec^{-1}/m^2$ near the center of the harshest spray.

Every type of nozzle used produced a different drop size spectrum. Changing nozzle pressure also altered the distribution of drop sizes for each nozzle. The present measurements demanded a method for determining a representative drop size at specified location in the spray for each nozzle and pressure. The Malvern Particle Sizer having a drop size measurement range of 2 to 1800 μm was utilized for this purpose. As the nozzle sprayed water across the laser beam of the Malvern system, a cone of light was diffracted behind each drop. The angle of diffraction for each of these light cones depends only on drop size regardless where the drop is located in the laser beam; the smaller the drop, the wider is the angle of diffraction. Diode rings detected the diffracted light cones corresponding to a range of drop sizes; the more drops of one size range in the beam, the more intense the light was upon its related diode ring. Several statistical diameters called mean diameters (including the Sauter mean diameter $d_{32}$ used in the present study) were calculated at the completion of a data run. Unfortunately, the Malvern spatial detection method precluded measurement of drop velocity and could not account for velocity in calculating the statistical diameters.

Drop velocities were measured using a two-dimensional grey scale optical array imaging probe which utilizes a temporal technique to measure the diameters and velocities of drops as they pass through an illuminated window of slicing planes. The first slice is defined as the time when the first photodiode is shadowed by the approaching drop, and the last slice is the time when the last shadow is detected after the drop has passed the illuminated window. Assuming the drop is spherical, the diameter is then recorded as the point when the largest shadow is detected. The time difference between the last slice and the first slice can then be calculated by dividing the number of slices that occurred through the drop by the slice rate. Once the diameter of the drop and the time it takes to pass through the slide plane are known, the velocity is simply determined as the diameter divided by the time.

### *Three-Dimensional Measurement of Temperature–Time Cooling Characteristics*

A highly instrumented preheating enclosure was developed to measure the transient temperature response of an aluminum block subject to a nonuniform spray cooling boundary. The block geometry was based on a numerical analysis of the quench transient and several design criteria. Since the temperature measurements were transient, it was necessary to ensure that the quench rate experienced by the block be several times slower than the time constant of the thermocouples. One method of slowing the quench rate was to decrease the thermal capacitance (i.e., mass) of the block. It was also desired that the surface of the block exposed to the spray be large enough to facilitate detecting the spatial variation in heat flux associated with the nonuniform spray field, yet small enough that no significant portions of the surface were outside of the spray field where the heat transfer coefficient could not be accurately defined. Since flat (oval pattern) sprays are commonly used for quenching aluminum extrusions, a rectangular surface was chosen which was completely contained within the spray field. The block size was also limited by the power of the electrical heating element required to bring the mass of aluminum up to test temperature in a reasonable time period. As many of the materials used in the heater construction were near or slightly over their maximum temperature limits for some tests, it was de-

cided to reduce the risk of burning these components by minimizing the heat-up period.

The block was fabricated from 99.4% aluminum (1100-0 series) since the thermal properties of this material could be carefully determined. The problems associated with using aluminum described for the steady state heating device used for local measurements were less significant with the block enclosure because the latter did not maintain very high temperatures for any significant time duration.

A schematic of the block preheating enclosure is shown in Figure 3. The block consisted of a 6.0 × 11.9 × 10.5 $cm^3$ rectangular aluminum block which provided a quench surface area of 71.9 $cm^2$. Transient block temperatures were measured with 14 type-T thermocouples made from 0.127 mm wires and set in 0.711 mm diameter holes drilled in planes parallel to the surface so as to minimize disturbance to isotherms. Type-T thermocouples were selected for their fast temperature response compared to all other common thermocouple types. A time constant of 0.20 msec was calculated based on an effective thermocouple bead diameter of 0.51 mm. In measuring the fastest cooling rate detected in the present study (approximately 225° C/sec), thermocouple response (based on four time constants) was estimated to lag the true temperature by 0.2° C. To further enhance the transient response, special care had to be taken during installation of the thermocouples to ensure excellent contact between the aluminum and the thermocouple bead.

Thermocouples were installed at two different planes within the block as shown in Figure 3. The layout of the thermocouple locations was chosen so as to maximize the sensitivity of the measurements to spray cooling nonuniformity. On the plane closest to the surface, temperatures were sensed at the center and near the corners of the block. One quadrant was more finely instrumented to detect small gradients in the surface heat transfer rate between the central axis and the edge. A fewer number of temperature probes were installed in the plane midway into the block since plan-wise temperature variations were dampened at that depth, causing a marked decrease in spatial sensitivity to surface temperature nonuniformity. An additional thermocouple was placed at the geometrical center of the block 2.5 cm from the bottom. This thermocouple was used for safety, to monitor the temperature in the block during preheating, and to establish when the block temperature had become uniform.

The heater casing was constructed out of G-7 fiberglass, a good insulating material capable of with

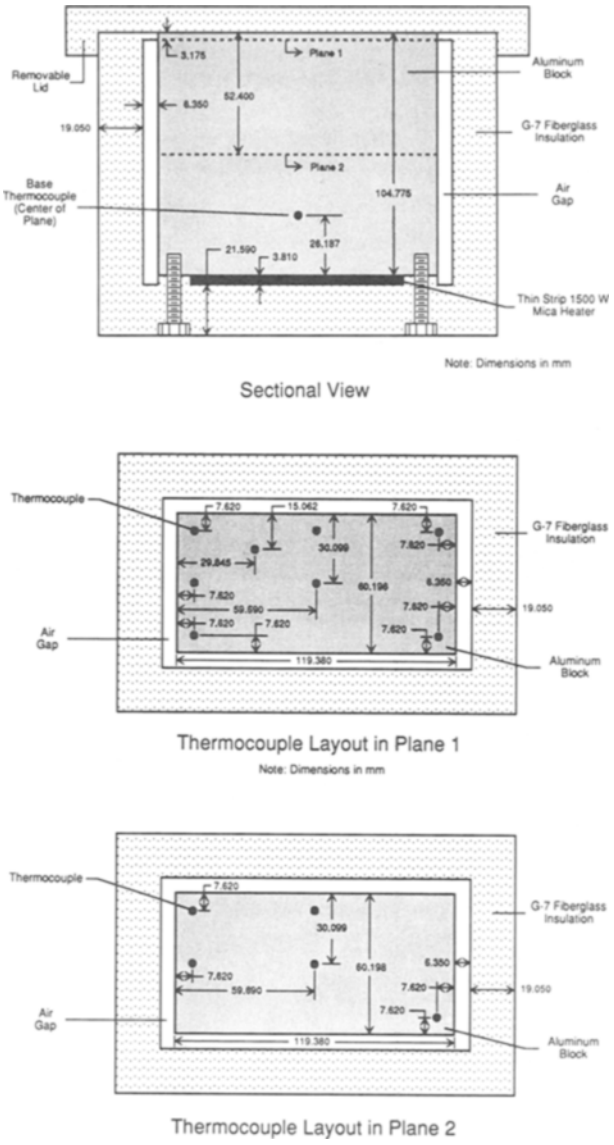


**Fig. 3.** Sectional views of the three-dimensional aluminum block and preheating enclosure.

standing surface temperatures as high as 400° C for short durations. Thermal insulation around the block was further enhanced by a 0.64 cm air gap which minimized aluminum contact with the G-7. The G-7 collar was machined with a 45 deg fillet, leaving a 0.32 cm gap at the top interface with the aluminum to permit expansion of the block. The void left at the interface was filled with silicone rubber to seal the aluminum block and heater from the harsh spray environment. Additionally, the entire exterior of the G-7 casing was coated with a thin layer of the silicone rubber to prevent water from penetrating the casing. A heater lid was used during preheating to shelter the aluminum surface from the spray until the desired

initial temperature had been reached uniformly throughout the block. The lid was removed quickly from the side at the onset of quench data acquisition, providing a nearly instantaneous application of the spray cooling boundary over the entire surface.

## Results and Discussion

### *Verification of the Spatial Independence of the Heat Transfer Correlations*

The first objective of the present study was to verify that the correlations developed by Mudawar and Valentine [9] were indeed spatially independent. To achieve this objective, a series of experiments were conducted using the smaller steady state heating device, Figure 2, and several carefully selected spray nozzles which were operated at various pressures and located at various distances from the quench surface. The water spray temperature was held constant at 23° C for the entire investigation.

Mudawar and Valentine correlated the heat transfer characteristics of a spray using local hydrodynamic parameters (i.e., $Q''$, $d_{32}$, and $U_m$). To simplify and reduce the size of their data matrix, all their local measurements were limited to the center of each spray. The present investigation involved similar local measurements, but obtained throughout the spray field. Figure 4 shows a quench curve obtained for a flat spray having the spray parameters $Q'' = 1.60 \times 10^{-3}$ m$^3$ sec$^{-1}$/m$^2$, $d_{32} = 148$ μm and $U_m = 19.6$ m/sec, which were measured at the position of the heating device, along the large axis of the oval spray field but away from the central axis.

Figure 4 shows agreement between the measured and predicted values even though the drop diameter (148 μm) is well below the range of diameters (405–1351 μm) recommended for using the correlations (see Table 1). Hence, local quench curves can be generated for every point on the quench surface using these correlations once the distributions of $Q''$, $d_{32}$ and $U_m$ are determined.

### *Spatial Distribution of Spray Hydrodynamic Parameters*

By obtaining local measurements of $Q''$, $d_{32}$, and $U_m$ at selected locations in the spray field, as shown schematically in Figure 5, a spatial distribution can be generated for each of these parameters. A plot of $Q''$ for a flat (oval) spray as a function of $X$ and $Y$ corresponding to the quench surface of the aluminum

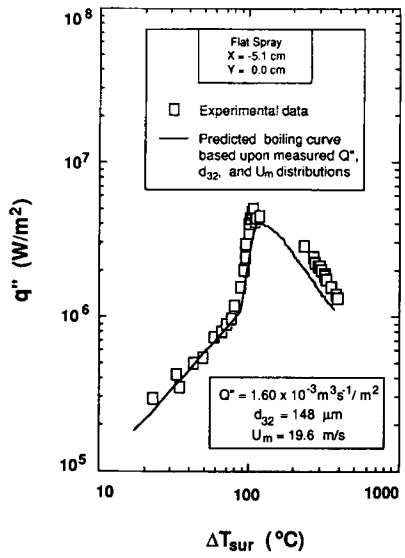


**Fig. 4.** Measured boiling curve compared with predictions based upon measured local hydrodynamic parameters.

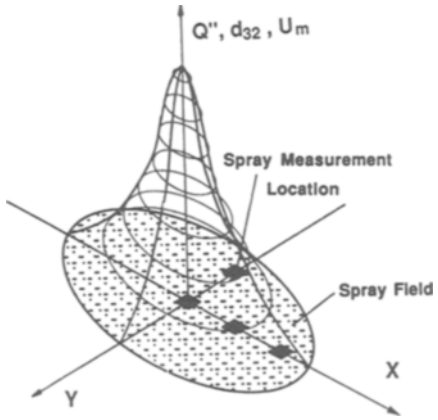


**Fig. 5.** Local hydrodynamic measurements made at discrete locations in the spray field.

block reveals a three-dimensional bell shaped curve as shown in Figure 6. The origin of the three-dimensional plot is located directly below the nozzle orifice. This is usually the location of highest volumetric flux. An exponential function of $X$ and $Y$ was found to represent well the asymmetric three-dimensional distribution of $Q''$ data shown in Figure 6 and the corresponding distributions of $d_{32}$ and $U_m$, as well as the distributions of these parameters for other spray types and conditions. The function has the form:

$$\Psi(X, Y) = A_0 e^{(A_1X + A_2Y + A_3X^2 + A_4XY + A_5Y^2)} \quad (1)$$

where $\Psi$ represents $Q''$, $d_{32}$, or $U_m$. Using the least square method of reducing deviation to determine

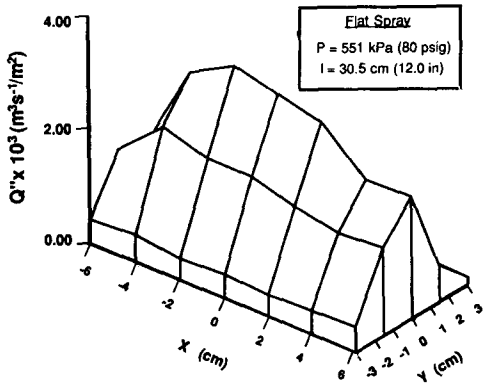


**Fig. 6.** Measured spatial distribution of volumetric spray flux.

the constants $A_0$ through $A_5$, the best fit of Eq. (1) to the volumetric flux data is illustrated in Figure 7(a). It is important to note that the curve fit is not sensitive to all of the irregularities in the volumetric flux distribution. It does, however, provide a good approximation to the local flux over a large portion of the sprayed surface area.

The mean drop diameter and drop velocity did not exhibit the steep gradient from the center to the edge of the spray that volumetric flux did. However, Eq. (1) demonstrated flexibility in representing these relatively flat distributions as well. Only a limited number of data points were necessary for the development of distribution functions for Sauter mean diameter, Figure 7(b), and mean drop velocity, Figure 7(c), compared to volumetric flux since the distributions of the former parameters were void of local excursion.

Recent studies by the authors have demonstrated the flexibility and universal applicability of Eq. (1) to fitting $Q''$, $d_{32}$, and $U_m$ data for many types of flat, full cone, and hollow cone sprays.

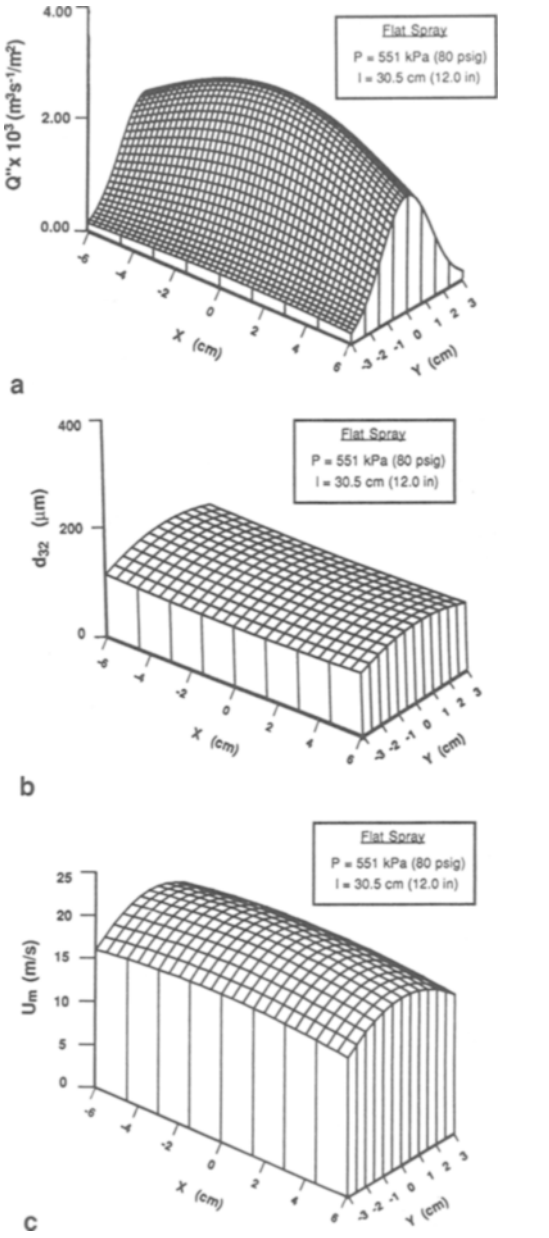


**Fig. 7.** Exponential curve fits to measured distributions of (a) volumetric spray flux, (b), Sauter mean diameter, and (c) mean drop velocity.

*Numerical Simulation of the Temperature Distribution in the Aluminum Block During the Quench*

The physical domain of the aluminum block used in the transient cooling experiment was simulated using PHOENICS, a commercially available finite difference software package. The material properties were input as functions of temperature and, as such, were allowed to vary during the transient response of the block to the quench.

The geometry was discretized nonuniformly by uniquely specifying locations of each grid in the $X$, $Y$, and $Z$ directions as shown in Figure 8. The dashed lines in this three-dimensional view represent the control volume interfaces. In the $X$ and $Y$ directions grids were first selected to coincide with thermocouple measurement locations. Afterwards grids were added to smooth out the discretized domain, making it as equally spaced as possible. In the $Z$ direction, which is the primary direction of heat flow, grids were spaced very finely near the sprayed surface, where large temperature gradients were expected, and more coarsely near the bottom. The grids closest

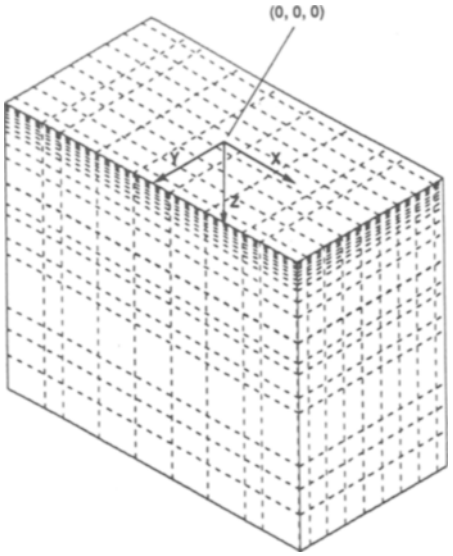


**Fig. 8.** Discretized three-dimensional aluminum block.

to the measurement planes were modified to exactly coincide with these locations. The time domain was discretized using a power law function with an exponent of 2. Initially a very fine time domain was needed since temperatures were changing rapidly. The first run would take 100 time steps for a total elapsed time of 10 sec. Following the sharp initial transient, larger time steps were simulated for 50 sec more. The initial condition for the simulation was a uniform block temperature which was measured just prior to the onset of the quench (i.e., before the lid was removed to expose the block surface to the spray).

The three-dimensional temperature distribution in the block was obtained by solving the heat diffusion equation

$$\frac{\partial^2 T}{\partial X^2} + \frac{\partial^2 T}{\partial Y^2} + \frac{\partial^2 T}{\partial Z^2} = \frac{1}{\alpha}\frac{\partial T}{\partial t} \qquad (2)$$

where $\alpha$ is the thermal diffusivity of aluminum. This equation was solved using PHOENICS by approximating the partial derivatives with finite difference equations.

The spray convection coefficient was calculated uniquely for each boundary grid. During the first numerical iteration, the location of each quench boundary grid relative to the central grid point set the local values of $Q''$, $d_{32}$, and $U_m$ based upon mathematical distribution functions developed for the particular spray configuration being simulated. By substituting the local values of the spray parameters in Mudawar and Valentine's local heat transfer correlations, a unique boiling curve was determined for every quench boundary node. The boiling curve was saved in computer memory so that, for the remainder of the calculations, knowledge of the boundary grid temperature alone would be sufficient to calculate a convection coefficient for that location.

The other five sides of the aluminum block were insulated in the actual experiment. However, the insulation was less than perfect, and some heat was lost through these boundaries. A simplified one-dimensional numerical model showed that, within the 60 sec window of the quench, the low conductivity of the insulation precluded any significant contribution of the insulating walls to heat dissipation from the block. Therefore, these boundaries were assumed perfectly insulated in the three-dimensional numerical simulations of this study.

### *Comparison of Numerical and Experimental Results for the Transient Response of the Aluminum Block*

The aluminum block was quenched by a flat spray having a spray angle of 51 deg, issuing with a back pressure of 551 kPa from a nozzle located 30.56 cm above the quench surface. This particular spray nozzle was selected for its large excursions in $Q''$, causing the largest deviation in the exponential curve fit for $Q''$ from experimental data compared to any other nozzle examined.

Figure 9 shows a comparison of the measured and predicted transient temperature response for two lo-

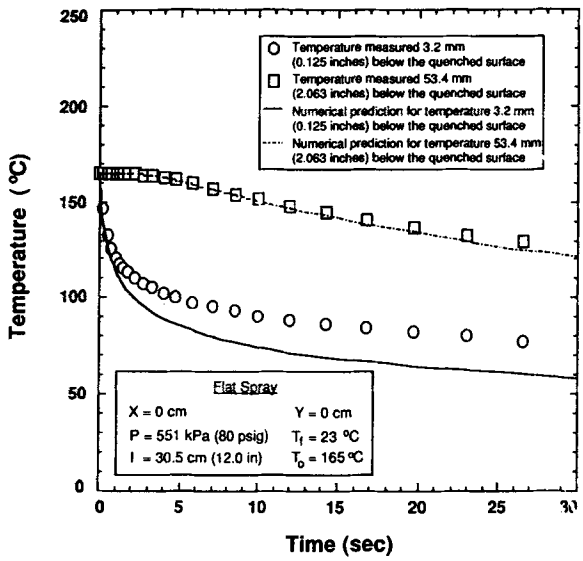


**Fig. 9.** Comparison of measured and numerically predicted temperature–time quench characteristics along the central axis of the block.

cations along the central axis ($X = 0$, $Y = 0$) of the aluminum block 3.2 and 53.4 mm below the quench surface. The predicted response is in excellent agreement for the latter point. Near the surface, there is good agreement during the first second of the response which corresponds to the transition and nucleate boiling regions largely responsible for determining the metallurgical properties of aluminum alloys during extrusion processes.

A deviation of the numerical predictions from the measured temperatures begins approximately when the convective boundary condition becomes dominated by single-phase liquid cooling which, as mentioned earlier, is insignificant to materials processing since the transition from nucleate boiling to single-phase liquid cooling occurs at very low surface temperatures. Small deviations in predicting temperatures corresponding to the single-phase regime occurred in experiments involving other types of spray nozzles as well. There are several possibilities for the source of this deviation. Although both the small steady state heating device used to develop the local quench correlations in Mudawar and Valentine's study and the large aluminum block used in the present study allow a liquid film to build up on the sprayed surface, the small surface area of the steady state heater is insufficient for heating the film as it moves across the surface. In the transition and nucleate boiling regimes it is expected that individual drops impact the surface and vaporize. Thus, there is little film buildup and heating and both measurements should provide nearly identical results. However, in the single-phase cooling regime the water drops lose their sensible energy upon impact but do not evaporate. Following impact, the drops coalesce with other drops to form a liquid film which flows across the sprayed surface. In the case of the large block, the film heats up as it moves towards the edge of the heated surface, rendering the convection due to drop impingement away from the central axis of the block less effective. The steady state heating device cannot account for the liquid film heating, therefore, the measured heat transfer rate is higher than that experienced by the three-dimensional block. This phenomenon may account for the faster transient response predicted by a numerical simulation which utilizes correlations for the quench surface based upon heat transfer results obtained with the steady state heating device.

Another reason for the small deviation between measured and predicted values is that the quench boundary conditions for the numerical results were based upon the exponential curve fits and not the true distribution of the spray hydrodynamic parameters. The agreement between the measured and predicted results is in fact an indication of the feasibility of the new technique considering that, for the particular test represented in Figure 9, the average absolute deviation of the exponential curve fit of the volumetric spray flux was 30.3% with local excursions as high as 50%, the highest deviation and excursion values encountered by the authors.

Figures 10(a) and (b) show comparisons of the measured temperatures and the corresponding numerical predictions for several locations along the

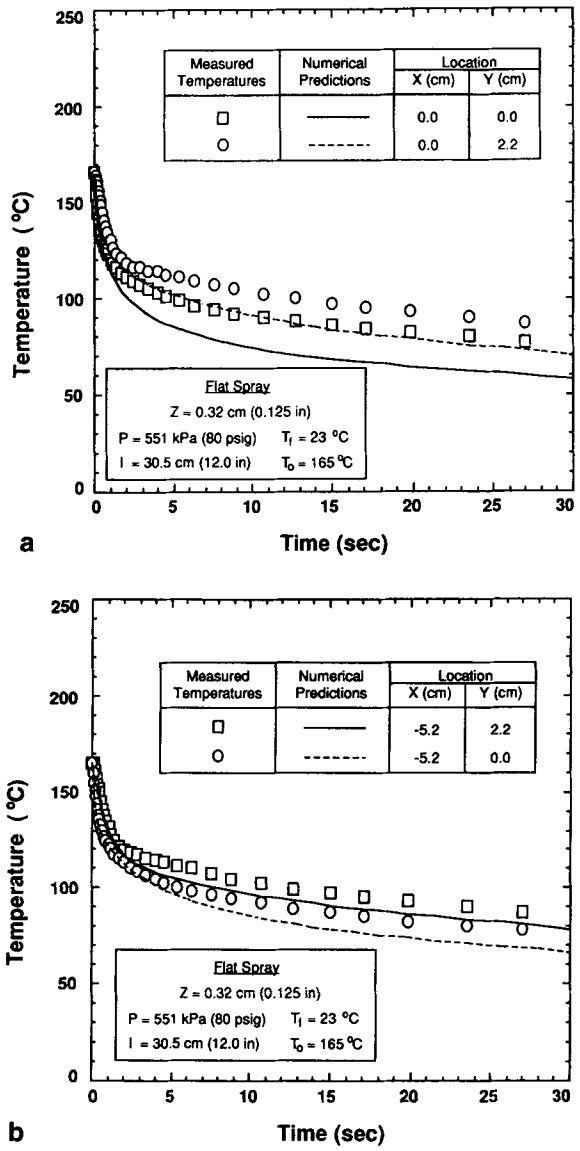


**Fig. 10.** Comparison of measured and numerically predicted temperature–time quench characteristics near the quench surface at the points (a) (0, 0, 0.32 cm) and (0, 2.2 cm, 0.32 cm); and (b) (−5.2 cm, 0, 0.32 cm) and (−5.2 cm, 2.2 cm, 0.32 cm).

major and minor axes of the spray field and near the quench surface. Since this is a flat spray oriented lengthwise along the quench surface, the largest variation in the heat transfer coefficient occurs across the width of the sprayed surface where the volumetric spray flux changes most drastically. The numerical predictions, although slightly deviant from data in the single-phase regime, are quite accurate in the transition and nucleate boiling regimes and follow the measured trends of decreasing cooling rate

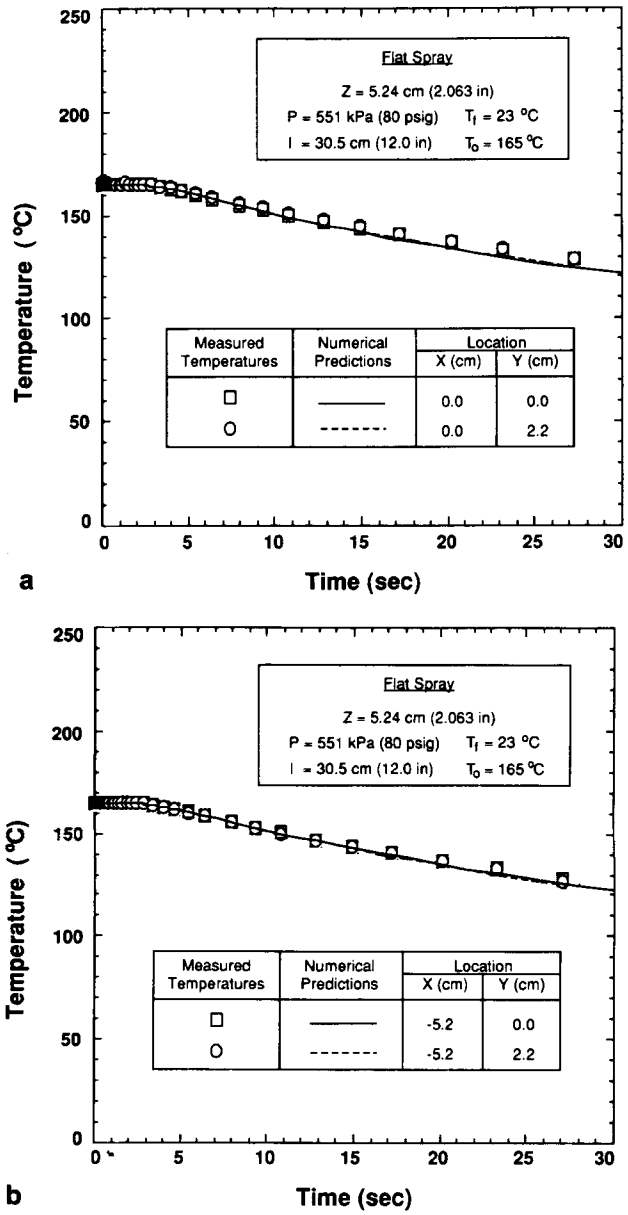


**Fig. 11.** Comparison of measured and numerically predicted temperature–time quench characteristics away from the quench surface at the points (a) (0, 0, 5.24 cm) and (0, 2.2 cm, 5.24 cm); and (b) (−5.2 cm, 0, 5.24 cm) and (−5.2 cm, 2.2 cm, 5.24 cm).

from the centerline ($Y$ = 0.0 cm) to the edge of the block ($Y$ = 2.2 cm). Figures 11(a) and (b) show excellent agreement between measured and predicted values for points away from the quench surface corresponding to $X$ and $Y$ locations identical to those of Figures 10(a) and (b), respectively.

It is important to note that, in all the experiments performed by the authors, the predicted quench rates were most accurate in the transition and nucleate boiling regimes which are most critical to the metallurgical properties of the aluminum part.

The numerical predictions of the present study prove that the combined use of the spray cooling correlations developed by Mudawar and Valentine, and the exponential curve fits to the hydrodynamic parameters of the spray, is a feasible approach to predicting the quench rates of aluminum products and to the optimization of spray cooling for more complex shapes as illustrated in Figure 1.

*Acknowledgments.* Financial support for this work by the Purdue University Engineering Research Center for Intelligent Manufacturing Systems and ALCOA is gratefully appreciated. The authors thank Messrs. Gerry Dail and William Author of ALCOA, and Rudolf Schick and Jerry Hagers of Spraying Systetms Co. for their valuable technical assistance.

## References

1. T.A. Deiters and I. Mudawar: *J. Heat Treating*, 1989, Vol. 7, pp. 9–18.
2. J.K. Brimacombe, P.K. Agarwal, L.A. Baptista, S. Hibbins, and B. Prabhakar: 63rd National Open Hearth and Basic Oxygen Steel Conf. Proc., 1980, Vol. 63, pp. 235–252.
3. L. Bolle and J.C. Moureau: Proc. of Two Phase Flows and Heat Transfer, 1976, Vol. III, NATO Advanced Study Institute, pp. 527–534.
4. L. Bolle and J.C. Moureau: Int. Conf. on Heat and Mass Transfer Metallurgical Processes, Dubrovnik, Yugoslavia, 1979, pp. 527–534.
5. K. Sasaki, Y. Sugitani and M. Kawasaki: *Testu-To-Hagane*, 1979, Vol. 65, pp. 90–96.
6. H. Muller and R. Jeschar: *Arch. Eisenhuttenwes*, 1973, Vol. 44, pp. 589–594.
7. L. Urbanovich, V. Goryaninov, V. Sevost'yanov, Y. Boev, V. Niskovskikh, A. Grachev, A. Sevost'yanov and V. Gur'ev: *Steel in the USSR*, 1981, Vol. 11, pp. 184–186.
8. U. Reiners, R. Jeschar, R. Scholz, D. Zebrowski and W. Reichelt: *Steel Research*, 1985, Vol. 56, pp. 239–246.
9. I. Mudawar and W.S. Valentine: *J. Heat Treating*, 1989, Vol. 7, pp. 107–121.

Received February 5, 1990.